

## RESEARCH ARTICLE

View Article Online  
View Journal | View Issue


Cite this: *Mater. Chem. Front.*,  
2018, 2, 603

Received 11th November 2017,  
Accepted 13th January 2018

DOI: 10.1039/c7qm00521k

rsc.li/frontiers-materials

# Calcium ion-assisted lipid tubule formation†

Sandra Jones, An Huynh, Yuan Gao and Yan Yu \*

Self-assembled lipid tubules are unique supramolecular structures in cell functions. Lipid tubules that are engineered *in vitro* are of great interest for technological applications ranging from the templated synthesis of nanomaterials to drug delivery. Herein, we report a study to create long lipid tubules from a mono-unsaturated lipid, 1-stearoyl-2-oleoyl-*sn*-glycero-3-phosphocholine (SOPC), due to the effect of calcium ions. We found that calcium ions at mM concentrations promote the self-assembly of SOPC lipids into inter-connected hollow lipid tubes that are  $\mu\text{m}$  thick and as long as a few millimeters. Higher calcium concentration leads to an increase in the numbers of lipid tubules formed, but has little effect on tubule diameter. Calcium ions also stabilize lipid tubules, which break up upon the removal of ions. We showed that the lipid tubule-promoting effect is general for divalent ions. We were able to vary the morphology of lipid tubules from thin tube to “strings of pearls” structures or increase the tubule thickness by mixing SOPC with other lipids of different spontaneous curvature effects. Our results reveal that the divalent charges of calcium ions and the asymmetric mono-unsaturated structure of SOPC acyl chains act in combination to cause the formation of lipid tubules.

## Introduction

Thin tubular membranes formed by the self-assembly of lipids are abundant structures within cells and sometimes between cells. Many intracellular organelles, including the trans-Golgi network, the endoplasmic reticulum, and the transverse tubular systems in muscle cells, consist largely of tubular membranes. The purpose of those tubular shaped organelle

domains remains a subject of debate, but it has been hypothesized that their hollow structure, high curvature and large total surface area make them preferred sites for protein accumulation and inter-organelle transport.<sup>1,2</sup> Lipid nanotubes, also known as tunneling nanotubes (TNTs), have also been found to form between cells to facilitate long-distance intercellular transport and signal communication. Ions, proteins, membrane vesicles and mitochondria can be transferred between cells through nanotube channels.<sup>3–8</sup> Viruses such as the human immunodeficiency virus (HIV) have also been shown to hijack the lipid tube network as a means to spread from an infected to a healthy cell.<sup>9,10</sup> In addition to their important natural roles in maintaining cell functions and in diseases, lipid tubules are of great interest for many materials engineering applications. For example, they have been developed for drug delivery because their large aspect ratio enables unique controlled release properties.<sup>11,12</sup> Lipid nanotubes have also been employed as templates for fabricating inorganic nanomaterials.<sup>13–19</sup> Because of these multiple areas of interest, extensive research efforts have been devoted to understanding the mechanisms of lipid tube formation and to finding a means for creating such membrane structures *in vitro*.

Lipid tubules generally form in one of two possible ways. The first way is through the self-assembly of lipids with the appropriate chemical structures or lipid composition. A limited number of lipids are known to be capable of spontaneously forming tubular structures. These mainly include glycolipids, lipids containing diacetylenic acyl chains, and mixtures of hydroxyl fatty acids.<sup>20–24</sup> A well-known example is the lipid

Department of Chemistry, Indiana University, Bloomington, Indiana 47405, USA.

E-mail: yy33@indiana.edu

† Electronic supplementary information (ESI) available: Fig. S1–S3. See DOI: 10.1039/c7qm00521k



Yan Yu

Prof. Yan Yu is currently an Assistant Professor in the Department of Chemistry at Indiana University–Bloomington. She received her PhD in Materials Science and Engineering at the University of Illinois at Urbana–Champaign in 2009 and completed postdoctoral training at the University of California – Berkeley in 2012. Prof. Yan Yu’s group is working on developing nanomaterial-enabled tools to measure and control cellular functions.

1,2-bis(10,12-tricosadiynoyl)-*sn*-glycero-3-phosphocholine (DC<sub>8,9</sub>PC), which forms chiral lipid tubules.<sup>21,24</sup> The second way that lipid tubules can form is through deformation of spherical lipid vesicles due to external causes, such as the interaction of proteins or the application of external forces. A wide variety of membrane-binding proteins have been shown to induce tubular protrusions from lipid vesicles, with the exact mechanism varying for different proteins.<sup>25–28</sup> We have shown previously that the interaction of cationic nanoparticles with lipid membranes causes tubulation and pearling of spherical lipid vesicles.<sup>29</sup> Similar effects have been found with the adsorption of polymers.<sup>30</sup> The transformation of lipid vesicles into nanotubes can also be induced by external forces from the application of electric fields,<sup>31,32</sup> fluid shear flow,<sup>33,34</sup> mechanical pulling,<sup>35,36</sup> or osmotic stress.<sup>37</sup> A recent study has demonstrated that light-induced structural changes of lipids lead to the formation of nanotubes from lipid vesicles.<sup>38</sup> The properties of the lipid nanotubes depend on the formation conditions. It is therefore important to explore in detail factors that may drive or influence the formation of lipid tubules, so that one can understand the formation mechanisms and develop ways to create lipid nanotubes of desirable features.

In this study, we investigated the formation of lipid tubules due to the effect of calcium ions (Ca<sup>2+</sup>). Ca<sup>2+</sup> ions play an indispensable role in a wide variety of cellular functions ranging from signal transduction to muscle contraction. Their binding to lipids has been shown to change the properties of lipid membranes, including the tilting angle of lipid headgroups, packing of lipid molecules, and spontaneous curvature and tension of lipid membranes.<sup>39–47</sup> But the effect of Ca<sup>2+</sup> on the formation of lipid tubules has been reported only in a few studies. In our previous study, we have shown that adding mM concentrations of Ca<sup>2+</sup> inhibits the tubulation and “pearling” of giant unilamellar vesicles (GUVs) induced by cationic nanoparticles.<sup>29</sup> Such an effect of Ca<sup>2+</sup> seems to reverse when the tubulation was induced by anionic instead of cationic nanoparticles.<sup>30</sup> A recent study has also reported that the local injection of Ca<sup>2+</sup> into GUVs triggers the formation of inward nanotube protrusions.<sup>48</sup> All three studies concern tubulation of existing spherical lipid vesicles. In contrast, we investigated in this study the self-assembly of lipid tubules. Our results show that Ca<sup>2+</sup> ions promote the self-assembly of a mono-unsaturated lipid, 1-stearoyl-2-oleoyl-*sn*-glycero-3-phosphocholine (SOPC), into inter-connected thin lipid tubules that can be as long as a few millimeters. Without Ca<sup>2+</sup> ions, SOPC lipids hardly form lipid tubules. We observed that higher Ca<sup>2+</sup> concentrations lead to the formation of more lipid tubules, but have little effect on the diameter of the tubules. Ca<sup>2+</sup> ions are also required in stabilizing lipid tubules, as removing them from the solution causes “pearling” and eventual break-up of the tubular membrane structure. We found that the combination of the divalent charges of Ca<sup>2+</sup> ions and the asymmetric mono-unsaturated structure of the SOPC acyl chains leads to lipid tubule formation. The morphology of the lipid tubules can be modulated by varying the lipid composition.

## Experimental

### Reagents

**Phospholipids** 1-stearoyl-2-oleoyl-*sn*-glycero-3-phosphocholine (SOPC), 1,2-dipalmitoyl-*sn*-glycero-3-phosphocholine (DPPC), and cholesterol were purchased from Avanti Polar Lipids (Alabaster, AL). Fluorescent lipid *N*-(4,4-difluoro-5,7-dimethyl-4-bora-3a,4a-diaza-*s*-indacene-3-propionyl)-1,2-dihexadecanoyl-*sn*-glycero-3-phosphoethanolamine, triethylammonium salt (BODIPY-DHPE) was obtained from Invitrogen (Carlsbad, CA). Round glass coverslips were purchased from Bioprotech, Inc. (Butler, PA). Ethylenediaminetetraacetic acid (EDTA) was obtained from Avantor Performance Materials (Center Valley, PA).

### Preparation of lipid tubules

A stock lipid solution of 1 mg mL<sup>−1</sup> of SOPC and 2 μg mL<sup>−1</sup> BODIPY-DHPE was prepared and stored in chloroform and used in all experiments. Glass coverslips were cleaned *via* sonication in an ethanol/water mixture (1 : 1, v/v) for five minutes, rinsed in water, and then etched with piranha solution (a mixture of 30% H<sub>2</sub>O<sub>2</sub> and sulfuric acid at a 1 : 3 volume ratio) for 15 minutes. After the coverslips were air dried, 6 μL of the SOPC stock solution was added onto the coverslips and formed a thin lipid film after chloroform evaporation. The lipid-coated coverslips were pre-hydrated in water moisture in a sealed glass beaker for 1 hour and then hydrated for 2 hours at room temperature in an aqueous solution containing 100 mM sucrose and various concentrations (0–20 mM) of CaCl<sub>2</sub>. In the EDTA experiments, 25 μL of 100 mM sucrose solution containing CaCl<sub>2</sub> or EDTA at indicated concentration was added to the imaging chamber during fluorescence imaging.

### Fluorescence imaging

Lipid tubules in imaging chambers were imaged using a Nikon Eclipse Ti microscope equipped with a 40× objective and an Andor iXon EMCCD camera. Confocal scanning fluorescence imaging was done on a Nikon A1R-A1 confocal microscope system equipped with a Nikon 100× oil-immersed objective and a Hamamatsu C11440 camera (Light Microscopy Imaging Center, Indiana University). Fluorescence images were analyzed using ImageJ imaging software (NIH).

## Results and discussion

The lipid used in our experiments was 1-stearoyl-2-oleoyl-*sn*-glycero-3-phosphocholine (SOPC). It is a zwitterionic lipid with two different acyl chains, one saturated and the other containing a double bond (Fig. 1a). To form lipid tubules, SOPC lipids were first dried on glass coverslips to become a thin film and then hydrated in an aqueous solution containing 100 mM sucrose and 10 mM CaCl<sub>2</sub>. Sucrose was added to speed up the gentle hydration of the lipid films, as shown in previous studies,<sup>49,50</sup> but it is not required for lipid self-assembly. Within 30 min of hydration, thin lipid tubules started to form spontaneously near the glass surface. The lipid tubules all aligned nearly parallel to the surface, but their orientation with

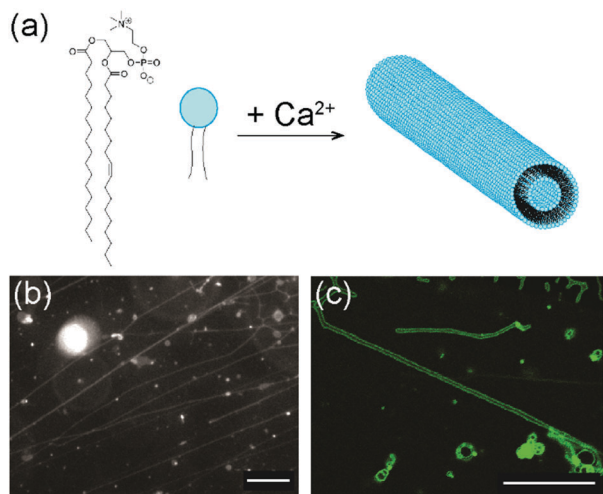


**Fig. 1** SOPC lipids self-assemble into tubular structures in an aqueous solution containing  $\text{Ca}^{2+}$ . (a) Schematic illustration of lipid tubules formed from SOPC lipids. Epifluorescence (b) and fluorescence confocal (c) images show multiple SOPC lipid tubules and their hollow structure. Scale bars: 20  $\mu\text{m}$ .

respect to each other was random. Some tubules were nearly parallel to each other, while others were inter-connected (Fig. 1b). Once formed, they remain stable for up to a day at room temperature, but can easily be broken up by a mechanical disturbance, such as shaking. Most lipid tubules are hollow cylindrical lipid membranes with a diameter of approximately 1  $\mu\text{m}$ , as shown in 3-D confocal fluorescence images (Fig. 1c). Their length varies from a few hundred  $\mu\text{m}$  to as long as a few millimeters. Some representative long lipid tubules are demonstrated in Fig. 2, in which multiple fluorescence images were “stitched” together to show the overall length of the lipid tubule network. As shown here, long lipid tubules are typically inter-connected. Small lipid globules, which appeared to be small lipid vesicles and aggregates, were found at many intersections.

To understand how SOPC lipids in dried films become hydrated and self-assemble into thin lipid tubules, we imaged the entire hydration process in real-time using fluorescence

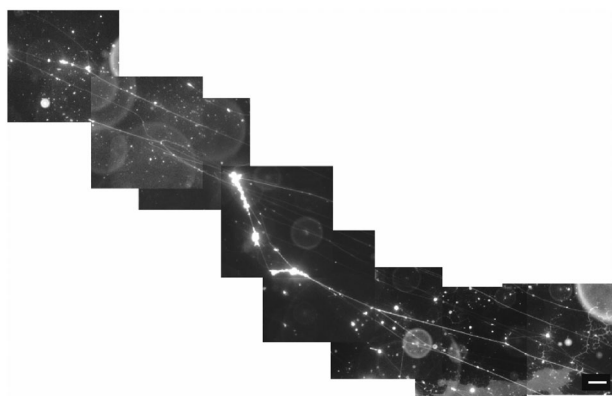


**Fig. 2** Stacked epifluorescence images show inter-connected lipid tubules that are  $>1$  mm in total length. Scale bar: 20  $\mu\text{m}$ .

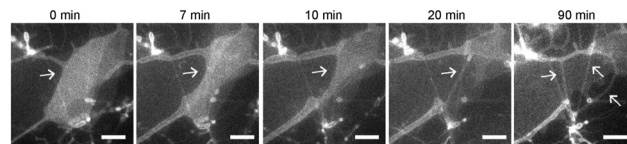


**Fig. 3** Fluorescence images show the formation of lipid tubules in a sucrose solution containing 20 mM  $\text{CaCl}_2$ . Arrows indicate where thin lipid films detach and transform into lipid tubules. Scale bars: 10  $\mu\text{m}$ .

microscopy (Fig. 3 and Movie S1, ESI<sup>†</sup>). We observed that the dried lipid films started to detach from the glass substrate within only a few minutes after hydration, and gradually transformed into thick hollow tubules of various diameters. As the hydration process proceeded, some thicker lipid tubules “branched” into multiple tubules of smaller diameters. Some others instead elongated to become thinner and longer tubules without “branching”. As the lipid films transformed into tubules, excess lipids were excluded as lipid globules that were either attached to intersections of lipid tubules or became dispersed in solution. From the real-time imaging, multiple stages in the self-assembly process are clear: the initial hydration of lipid films, lipid film detachment, transformation of lipid films into hollow tubules, and a spontaneous adjustment of the tubule morphology.

We next investigated the effect of  $\text{Ca}^{2+}$  concentration on the formation of lipid tubules. When  $\text{Ca}^{2+}$  was not present in the solution, only a small number of lipid tubules were observed, but more lipid tubules were formed as  $[\text{Ca}^{2+}]$  was increased gradually up to 20 mM (Fig. S1, ESI<sup>†</sup>). In contrast, we found that the concentration of  $\text{Ca}^{2+}$  had only a small effect on the diameter of the lipid tubules (Fig. 4). The average diameter of individual lipid tubules, measured in wide-field fluorescence images, remained between  $\approx 0.9$  and 1.1  $\mu\text{m}$  at  $\text{Ca}^{2+}$  concentrations of 0 to 5 mM, and it only slightly increased to  $\approx 1.3$ –1.5  $\mu\text{m}$  at  $\text{Ca}^{2+}$  concentrations of 10 and 20 mM.

In addition to the effect of  $\text{Ca}^{2+}$  on the formation of SOPC lipid tubules, we also sought to investigate whether or not  $\text{Ca}^{2+}$

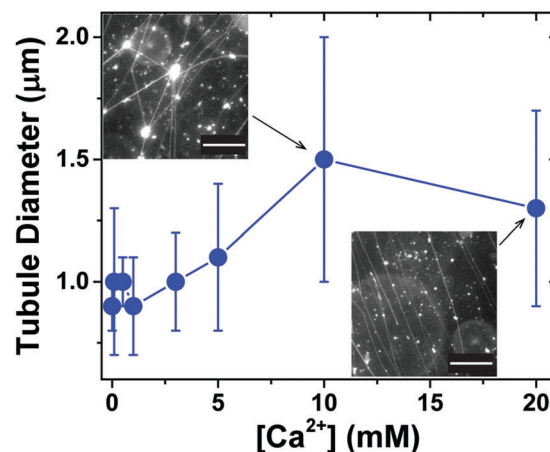


**Fig. 4** Effect of  $\text{Ca}^{2+}$  concentration on the diameter of lipid tubules. Error bars represent standard deviation. The insets show representative epifluorescence images of lipid tubules formed at  $[\text{Ca}^{2+}] = 10$  mM and  $[\text{Ca}^{2+}] = 20$  mM, respectively. Scale bars: 20  $\mu\text{m}$ .



ions are required for stabilizing the tubule structures once they are formed. In the experiments, we formed lipid tubules in a sucrose solution containing 10 mM  $\text{CaCl}_2$ , and then added 25  $\mu\text{L}$  of a sucrose solution containing 100 mM EDTA near the lipid tubules. EDTA was used because it chelates with  $\text{Ca}^{2+}$  and was expected to remove or reduce the concentration of  $\text{Ca}^{2+}$  near the outer membrane of the lipid tubules. We observed that the lipid tubules underwent a dramatic shape transformation within seconds after the addition of EDTA: they appeared “rippled”, transformed into a structure resembling a string of pearls, and then eventually broke up into small individual lipid globules (Fig. 5a). To test whether the lipid tubules were destabilized by mechanical disturbance from the local injection of solution, we injected 25  $\mu\text{L}$  of a sucrose solution containing 10 mM  $\text{CaCl}_2$  before adding EDTA. The lipid tubules remained stable under the influence of the fluid flow, indicating that the observed shape transformation of lipid tubules was not caused by the injection of EDTA solution. We also performed control experiments to exclude the possible effect of osmotic stress on the EDTA-induced lipid tubule destabilization. In the control experiments, an equivalent volume of a sucrose solution containing 100 mM  $\text{CaCl}_2$  instead of 100 mM EDTA was added to the lipid tubule medium. Despite the higher concentration of  $\text{Ca}^{2+}$  added locally, no changes to the morphology of the lipid tubules were observed, confirming that the lipid tubule break-up is not due to the osmotic stress effect (Fig. 5b). These results together demonstrate that the removal of  $\text{Ca}^{2+}$  outside of the lipid tubules destabilizes the structure of SOPC lipid tubules and induces them to transform from hollow tubes into lipid globules. We have shown previously that adsorption of cationic nanoparticles on one side of lipid membranes can induce a mismatch in membrane spontaneous curvature, which causes spherical vesicles to change shape into long “strings of pearls” at 0.01 nM concentration of nanoparticles and break up into individual smaller vesicles when the nanoparticle concentration increases to 1 nM.<sup>29</sup> Here, the lipid tubules appeared

to undergo a similar shape transformation. This led us to speculate that a spontaneous curvature effect is also involved in the destabilization of lipid tubules. Studies have shown that divalent cations, such as  $\text{Ca}^{2+}$ , bind to dipolar headgroups of zwitterionic lipids.<sup>39,51</sup> The strong binding of  $\text{Ca}^{2+}$  changes the tilting angle of the lipid head groups, which consequently may change the spontaneous curvature of lipids and induce lateral compression of the lipid bilayer.<sup>39–47</sup> Our results suggest that the presence of  $\text{Ca}^{2+}$  on both sides of the lipid membrane is required for maintaining the large curvature of the lipid tubules. It is possible that the removal of  $\text{Ca}^{2+}$  from one side of the lipid bilayer creates a mismatched spontaneous curvature, causing the lipid tubules to collapse.

We then asked whether lipid tubules would still form if  $\text{Ca}^{2+}$  was replaced by some other types of cations. When  $\text{MgCl}_2$  was added to the sucrose hydration buffer in place of  $\text{CaCl}_2$ , thin lipid tubules were formed at  $[\text{Mg}^{2+}] = 5 \text{ mM}$  and 20 mM, but fewer tubules were observed than with the same concentration of  $\text{Ca}^{2+}$  (Fig. S2, ESI<sup>†</sup>). The slightly lesser tubule forming effect of  $\text{Mg}^{2+}$  agrees with a previous report that  $\text{Ca}^{2+}$  is more effective in inducing lipid clustering in phosphatidic acid-phosphatidylcholine membranes than  $\text{Mg}^{2+}$ .<sup>52</sup> Unlike  $\text{Ca}^{2+}$  and  $\text{Mg}^{2+}$  ions, the presence of  $\text{Na}^+$  or  $\text{Al}^{3+}$  did not promote the formation of lipid tubules. The results demonstrate that divalent cations are critical for the formation and stability of the SOPC lipid tubules.

In addition to the effect of  $\text{Ca}^{2+}$  ions, we also noticed that the asymmetric structure of the acyl chains of SOPC is required for the lipid tubule formation, as the lipid 1,2-dioleoyl-*sn*-glycero-3-phosphocholine (DOPC), which is structurally similar to SOPC except that it has two identical mono-unsaturated acyl chains, only formed spherical lipid vesicles under the same experimental conditions. The results together led us to hypothesize that the membrane spontaneous curvature plays a crucial role in determining the formation and morphology of the lipid tubules. Because the spontaneous curvature of a lipid membrane is a



**Fig. 5** Effect of  $\text{Ca}^{2+}$  on the stability of lipid tubules. (a) Removal of  $\text{Ca}^{2+}$  by the addition of EDTA destabilizes the lipid tubules. (b) Lipid tubules remain stable in control experiments, in which an aqueous  $\text{CaCl}_2$  solution was added instead of EDTA solution of the same concentration. Scale bars: 20  $\mu\text{m}$ .

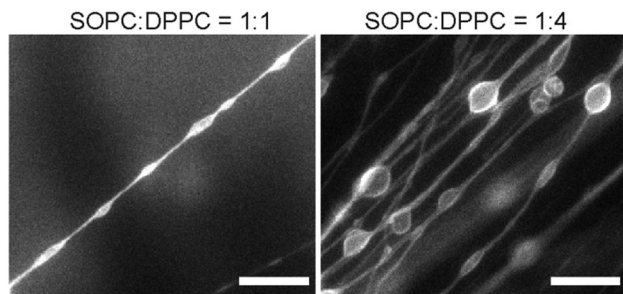


Fig. 6 Fluorescence images showing membrane structures formed from SOPC/DPPC lipid mixtures. Scale bars: 20  $\mu\text{m}$ .

collective property due to the interactions between individual lipid molecules, we speculate that mixing lipids of different spontaneous curvatures can lead to changes in the overall spontaneous curvature of the membrane and thus the morphology of lipid tubules. We tested this hypothesis by mixing SOPC with other lipids of different spontaneous curvatures. We first mixed SOPC with 1,2-dipalmitoyl-*sn*-glycero-3-phosphocholine (DPPC) at various molar ratios. DPPC is expected to have a significantly more positive lipid curvature than that of SOPC at room temperature due to its two saturated acyl chains.<sup>53</sup> Lipid films obtained from the SOPC/DPPC mixtures were hydrated at 60 °C, a temperature higher than the gel-to-liquid phase transition of both DPPC and SOPC, and were then imaged at room temperature. When SOPC and DPPC were mixed at either a 1:1 or 1:2 molar ratio, straight and long lipid tubules were no longer observed. Instead, we found membrane structures that resemble long strings of “pearls”, in which elongated vesicles were connected *via* lipid tubules (Fig. 6). The elongated vesicles became larger and more round with a higher content of DPPC. We did not observe large-scale phase separation of the SOPC and DPPC lipids, judging from the relatively homogeneous distribution of fluorescent lipids in the “pearling” membrane strings. Due to the diffraction limit, we could not identify in the fluorescence images whether microscale lipid segregation occurred. In a separate experiment, we mixed SOPC with another curvature-modulating molecule, cholesterol. Cholesterol has been shown to induce a negative curvature when mixed with lipids that have unsaturated acyl chains, but induce a positive curvature in the presence of saturated acyl chains.<sup>53,54</sup> We observed that the addition of a small percentage of cholesterol (5 mol% and 10 mol%) led to the formation of thicker lipid tubules (Fig. S3, ESI<sup>†</sup>). The results here demonstrate that the lipid tubule morphology can be varied by changing the membrane composition, and confirm the hypothesis that the membrane spontaneous curvature plays a crucial role in determining the formation and morphology of the lipid tubules.

## Conclusions

Here we investigated the role of calcium ions in the formation of lipid tubules from SOPC, a mono-unsaturated lipid. By using real-time fluorescence imaging, we directly observed the

dynamic process by which SOPC lipids self-assemble into long inter-connected  $\mu\text{m}$ -thick lipid tubules from dried lipid films. We found that higher  $\text{Ca}^{2+}$  concentrations promote increased formation of lipid tubules, but have little effect on the diameter of the tubules formed. Once lipid tubules are formed in such a medium,  $\text{Ca}^{2+}$  ions stabilize them. The removal of  $\text{Ca}^{2+}$  from the solution causes the tubules to ripple and eventually break up into small lipid globules. In general, the formation of lipid tubules requires the presence of divalent cations, but  $\text{Mg}^{2+}$  leads to a lower abundance of lipid tubules formed than  $\text{Ca}^{2+}$ . We were able to control the formation and morphology of the lipid tubules by mixing SOPC with lipids of different spontaneous curvatures. For example, mixing SOPC with DPPC leads to the formation of “pearl string” like membrane structures, whereas adding cholesterol resulted in thicker lipid tubules. Based on the results, we propose that  $\text{Ca}^{2+}$  ions facilitate lipid tubule formation in SOPC because their binding to the lipid headgroups changes its spontaneous curvature. This spontaneous curvature effect combined with the unique mono-unsaturated structure of lipids is necessary for stabilizing the large curvature of the lipid tubules. Given the significance of calcium ions in cell functions and the abundance of tubular membrane structures in biological systems, our study suggests that calcium ions might potentially play an important role in the formation and stabilization of the tubular subcellular structures.

## Conflicts of interest

There are no conflicts to declare.

## Acknowledgements

We thank Dr Jim Powers of the IUB Light Microscopy Imaging Center for assistance with confocal fluorescence imaging. This work was supported by the National Science Foundation, Division of Chemical, Bioengineering, Environmental, and Transport Systems (Grant No. 1705384) and Indiana University.

## References

- 1 H. H. Mollenhauer and D. J. Morre, *Histochem. Cell Biol.*, 1998, **109**, 533–543.
- 2 A. R. English and G. K. Voeltz, *Cold Spring Harbor Perspect. Biol.*, 2013, **5**, a013227.
- 3 B. Önfelt, S. Nedvetzki, R. K. P. Benninger, M. A. Purbhoo, S. Sowinski, A. N. Hume, M. C. Seabra, M. A. A. Neil, P. M. W. French and D. M. Davis, *J. Immunol.*, 2006, **177**, 8476.
- 4 D. M. Davis and S. Sowinski, *Nat. Rev. Mol. Cell Biol.*, 2008, **9**, 431–436.
- 5 S. C. Watkins and R. D. Salter, *Immunity*, 2005, **23**, 309–318.
- 6 G. P. Dubey and S. Ben-Yehuda, *Cell*, 2011, **144**, 590–600.
- 7 D. Wittig, X. Wang, C. Walter, H. H. Gerdes, R. H. Funk and C. Roehlecke, *PLoS One*, 2012, **7**, e33195.

- 8 A. Rustom, R. Saffrich, I. Markovic, P. Walther and H. H. Gerdes, *Science*, 2004, **303**, 1007–1010.
- 9 K. Gousset, E. Schiff, C. Langevin, Z. Marijanovic, A. Caputo, D. T. Browman, N. Chenouard, F. de Chaumont, A. Martino, J. Enninga, J. C. Olivo-Marin, D. Mannel and C. Zurzolo, *Nat. Cell Biol.*, 2009, **11**, 328–336.
- 10 S. Sowinski, C. Jolly, O. Berninghausen, M. A. Purbhoo, A. Chauveau, K. Kohler, S. Oddos, P. Eissmann, F. M. Brodsky, C. Hopkins, B. Onfelt, Q. Sattentau and D. M. Davis, *Nat. Cell Biol.*, 2008, **10**, 211–219.
- 11 J. M. Schnur, R. Price and A. S. Rudolph, *J. Controlled Release*, 1994, **28**, 3–13.
- 12 A. S. Rudolph, G. Stilwell, R. O. Cliff, B. Kahn, B. J. Spargo, F. Rollwagen and R. L. Monroy, *Biomaterials*, 1992, **13**, 1085–1092.
- 13 Y. Wang, S. Ma, Y. Su and X. Han, *Chem. – Eur. J.*, 2015, **21**, 6084–6089.
- 14 Y. Wang, S. Ma, Q. Li, Y. Zhang, X. Wang and X. Han, *ACS Sustainable Chem. Eng.*, 2016, **4**, 3773–3779.
- 15 P. Gao, C. Zhan and M. Liu, *Langmuir*, 2006, **22**, 775–779.
- 16 S. Baral and P. Schoen, *Chem. Mater.*, 1993, **5**, 145–147.
- 17 Y. Zhou and T. Shimizu, *Chem. Mater.*, 2008, **20**, 625–633.
- 18 A. J. Patil, E. Muthusamy, A. M. Seddon and S. Mann, *Adv. Mater.*, 2003, **15**, 1816–1819.
- 19 B. Yang, S. Kamiya, Y. Shimizu, N. Koshizaki and T. Shimizu, *Chem. Mater.*, 2004, **16**, 2826–2831.
- 20 K. Akiyoshi, A. Itaya, S.-I. M. Nomura, N. Ono and K. Yoshikawa, *FEBS Lett.*, 2003, **534**, 33–38.
- 21 M. S. Spector, K. R. K. Easwaran, G. Jyothi, J. V. Selinger, A. Singh and J. M. Schnur, *Proc. Natl. Acad. Sci. U. S. A.*, 1996, **93**, 12943–12946.
- 22 S. Kamiya, H. Minamikawa, J. H. Jung, B. Yang, M. Masuda and T. Shimizu, *Langmuir*, 2005, **21**, 743–750.
- 23 J.-P. Douliez, C. Gaillard, L. Navailles and F. Nallet, *Langmuir*, 2006, **22**, 2942–2945.
- 24 A. S. Jacques, H. Georger, R. R. Price, J. M. Schnur, P. Yager and P. E. Schoen, *J. Am. Chem. Soc.*, 1982, **109**, 6169.
- 25 A. Koth, D. Appelhans, D. Robertson, B. Tiersch and J. Koetz, *Soft Matter*, 2011, **7**, 10581–10584.
- 26 H. Liu, G. D. Bachand, H. Kim, C. C. Hayden, E. A. Abate and D. Y. Sasaki, *Langmuir*, 2008, **24**, 3686–3689.
- 27 M. Simunovic, C. Mim, T. C. Marlovits, G. Resch, V. M. Unger and G. A. Voth, *Biophys. J.*, 2013, **105**, 711–719.
- 28 J. C. Stachowiak, C. C. Hayden and D. Y. Sasaki, *Proc. Natl. Acad. Sci. U. S. A.*, 2010, **107**, 7781–7786.
- 29 Y. Yu and S. Granick, *J. Am. Chem. Soc.*, 2009, **131**, 14158–14159.
- 30 I. Gozen, C. Billerit, P. Dommersnes, A. Jesorka and O. Orwar, *Soft Matter*, 2011, **7**, 9706–9713.
- 31 C. Zhu, Y. Zhang, Y. Wang, Q. Li, W. Mu and X. Han, *Chem. – Eur. J.*, 2016, **22**, 2906–2909.
- 32 H. Bi, D. Fu, L. Wang and X. Han, *ACS Nano*, 2014, **8**, 3961–3969.
- 33 C. Hentrich and J. W. Szostak, *Langmuir*, 2014, **30**, 14916–14925.
- 34 Y. Sekine, K. Abe, A. Shimizu, Y. Sasaki, S.-I. Sawada and K. Akiyoshi, *RSC Adv.*, 2012, **2**, 2682–2684.
- 35 J. E. Reiner, R. Kishore, C. Pfefferkorn, J. Wells, K. Helmersen, P. Howell, W. Vreeland, S. Forry, L. Locascio, D. Reyes-Hernandez and M. Gaitan, *Proc. SPIE 5514, Optical Trapping and Optical Micromanipulation*, 2004.
- 36 M. Karlsson, K. Sott, A.-S. Cans, A. Karlsson, R. Karlsson and O. Orwar, *Langmuir*, 2001, **17**, 6754–6758.
- 37 P. Rangamani, D. Zhang, G. Oster and A. Q. Shen, *J. R. Soc., Interface*, 2013, **10**, 20130637.
- 38 C. Pernpeintner, J. A. Frank, P. Urban, C. R. Roeske, S. D. Pitzl, D. Trauner and T. Lohmüller, *Langmuir*, 2017, **33**, 4083–4089.
- 39 A. Melcrova, S. Pokorna, S. Pullanchery, M. Kohagen, P. Jurkiewicz, M. Hof, P. Jungwirth, P. S. Cremer and L. Cwiklik, *Sci. Rep.*, 2016, **6**, 38035.
- 40 L. Herbet, C. A. Napolitano and R. V. McDaniel, *Biophys. J.*, 1984, **46**, 677–685.
- 41 R. J. Clarke and C. Lüpfer, *Biophys. J.*, 1999, **76**, 2614–2624.
- 42 P. T. Vernier, M. J. Ziegler and R. Dimova, *Langmuir*, 2009, **25**, 1020–1027.
- 43 A. Cordomi, O. Edholm and J. J. Perez, *J. Phys. Chem. B*, 2008, **112**, 1397–1408.
- 44 H. Binder and O. Zschörnig, *Chem. Phys. Lipids*, 2002, **115**, 39–61.
- 45 R. A. Böckmann and H. Grubmüller, *Angew. Chem., Int. Ed.*, 2004, **43**, 1021–1024.
- 46 G. Pabst, A. Hodzic, J. Strancar, S. Danner, M. Rappolt and P. Lagner, *Biophys. J.*, 2007, **93**, 2688–2696.
- 47 S. Garcia-Manyes, G. Oncins and F. Sanz, *Biophys. J.*, 2005, **89**, 1812–1826.
- 48 B. Ali Doosti, W. Pezeshkian, D. S. Bruhn, J. H. Ipsen, H. Khandelia, G. D. M. Jeffries and T. Lobovkina, *Langmuir*, 2017, **33**, 11010–11017.
- 49 K. Akashi, H. Miyata, H. Itoh and K. Kinoshita, Jr., *Biophys. J.*, 1998, **74**, 2973–2982.
- 50 K. Tsumoto, H. Matsuo, M. Tomita and T. Yoshimura, *Colloids Surf., B*, 2009, **68**, 98–105.
- 51 M. Roux and M. Bloom, *Biochemistry*, 1990, **29**, 7077–7089.
- 52 T. Ito and S.-I. Ohnishi, *Biochim. Biophys. Acta*, 1974, **352**, 29–37.
- 53 B. Kollmitzer, P. Heftberger, M. Rappolt and G. Pabst, *Soft Matter*, 2013, **9**, 10877–10884.
- 54 A. J. Sodt, R. M. Venable, E. Lyman and R. W. Pastor, *Phys. Rev. Lett.*, 2016, **117**, 138104.